Semicond. Sci. Technol. **23** (2008) 105020 (5pp) doi:10.1088/0268-1242/23/10/105020

Optical behaviour of ion beam sputtered a-Si thin films

Koppolu Uma Mahendra Kumar and M Ghanashyam Krishna

School of Physics, University of Hyderabad, Hyderabad-500 046, India

E-mail: mgksp@uohyd.ernet.in

Received 15 May 2008, in final form 19 August 2008
Published 22 September 2008
Online at stacks.iop.org/SST/23/105020

Abstract

Pure amorphous silicon thin films have been deposited by ion beam sputtering onto borosilicate glass substrates at ambient temperature. Optical constants were derived from spectral transmittance measurements in the range of 350–2500 nm. All the samples, regardless of thickness, show a Raman peak centred between 460 and 480 cm^{-1}. The root-mean-square variation in the bond angles, $\Delta\theta$, obtained from Raman spectra, indicates the presence of relatively good short range order in amorphous silicon thin films. The refractive index at 1.4 eV decreases from 4.35 to 3.52 with an increase in thickness from 30 to 130 nm. The band gap varies with thickness and at a thickness of 130 nm the band gap is 1.3 eV, which increases to 1.8 eV at 30 nm. The narrow band gap values of ion beam sputtered a-Si thin films indicate that they can be explored for photovoltaic applications.

(Some figures in this article are in colour only in the electronic version)

1. Introduction

In the last two decades, amorphous hydrogenated silicon (a-Si:H) has been one of the most popular photovoltaic materials, after the first report on the growth of amorphous silicon by Chittick *et al* [1]. Later, a-Si:H has been used in a wide variety of device elements such as transistors, active display elements and large-area photo detectors [2, 3]. There are, however, some major disadvantages that a-Si:H suffers from that have limited its applicability in recent years, including the problem of instability after illumination (the Staebler–Wronski effect) [4]. Polycrystalline-silicon (poly-Si) has emerged as an alternative to a-Si. It is observed that as-deposited poly-Si generally has wide grain-size distribution. This affects the electrical properties of the device resulting in large minority leakage currents. In order to minimize the leakage currents and decrease the product cost, efforts are being made to find new methods to grow large grains with narrow size distributions and usage of inexpensive substrates such as glass and polymers. These above requirements can be met by introducing an additional step in the fabrication, i.e., recrystallization. However, the recrystallization temperatures are higher than the melting point of glass. This has led to the development of metal-induced crystallization as a viable method of poly-Si (MIC-Si) growth on glass and other cheap substrates. The poly-Si, thus formed, has yet to meet the device quality due to the presence of metal impurities. Defect-free (less dangling bond density), pure a-Si offers many advantages over a-Si:H, poly-Si and MIC-Si.

- Low temperature production.
- Almost every kind of substrate can be used.
- Doping of a-Si is easier.

Hence there has been a recent resurgence of interest in the preparation and characterization of defect-free unhydrogenated a-Si.

The aim of the present work is to explore the possibility of applying ion beam sputtering for the growth of pure a-Si on glass to meet the above-mentioned advantages. Ion beam sputtering offers many advantages; avoiding the use of toxic gases (used in chemical vapour based deposition techniques), greater control over the surface properties of the film as the substrates are isolated from the plasma, and independent control over incident beam energy, angle of incidence and current density of the neutralized ion beam. The effect of incident ion beam energy and thickness on the optical constants of very thin films of a-Si deposited onto borosilicate glass (BSG) substrates and their structural properties derived from Raman spectroscopy are presented.

2. Experimental details

Amorphous silicon thin films are grown on borosilicate glass substrates in a home-built ion beam deposition system evacuated by a turbo molecular pump (TMP). The dc ion source (DC25 of Oxford Applied Research, UK) is a Kaufmann-type ion source capable of producing ion beams of 2.5 cm in diameter with beam energy of up to 1.5 keV. The ions are extracted and accelerated by applying a suitable potential to a dual-grid ion extraction system. The deposition chamber was evacuated to a base pressure of 5×10^{-7} Torr before introducing argon gas into the system. The pressure during deposition is 5×10^{-4} Torr. The substrates are held at room temperature during deposition, and substrates are mounted on a substrate holder, which is 8 cm from the substrate and source axis.

Spectral transmittance is measured in the wavelength range 350–2500 nm by means of a dual-beam spectrophotometer (UV-VIS-NIR, model V-570, Jasco, Japan) having a resolution limit of 0.2 nm and a sampling interval of 2 nm. All the samples were measured at the same incidence angle of $6.0^\circ \pm 0.1$ in order to avoid any fringe shift due to angular discrepancy. The transmitted intensities were measured at accuracy better than 0.3%. Films of thickness in the range 30–130 nm were deposited, and their refractive indices and absorption coefficients were derived from the measured spectral transmission using the envelope technique [5]. For lower thickness films a computer code 'PUMA' [6] was used to determine the optical constants of thinner films.

The Raman spectra were recorded in air using an argon-ion laser in the back scattering geometry in a JY-ISA T64000 spectrometer equipped with an Olympus BX40 confocal microscope and 100× objective (1 μm diameter focal spot size) with a liquid nitrogen cooled charge coupled device (CCD) detector. The spectral components coming from the amorphous and crystalline components were de-convoluted and related to Raman shifts and peak broadening. After correcting for the base line, a Voigt-like function was used for curve fitting the Raman spectra. Care was taken to optimize the parameters of the He–Ne laser, so that it does not induce onset of crystallization in the sample. The phase content within the samples was investigated in a spectral region of 400–600 cm^{-1} with an irradiation time of 300 s.

3. Results and discussion

The Raman central frequency for a-Si varies from 460 cm^{-1} to 480 cm^{-1} depending on the local order of the a-Si. The substrate effects were ruled out using methods described by Iqbal *et al* [7]. An initial comparison with thermally evaporated films was also made, and is shown in figures 1(*a*) and (*b*). The Raman signal from 400 to 600 cm^{-1} was modelled using a Voigt-like function in order to find the central Raman frequency and peak width as they have correlation with structural properties.

Thermally evaporated a-Si on glass showed a Raman peak centred at 472 cm^{-1} with a FWHM of 61 cm^{-1}. This particular position of Raman frequency signifies the presence of amorphous clusters consisted of approximately 200 silicon atoms [8]. Figure 1(*b*) shows the Raman spectra of ion beam sputtered silicon thin film, again on glass held at room temperature, with the incident beam energy of 600 eV. The central Raman frequency shifts towards higher wave numbers of 483 cm^{-1}, i.e. towards the 520 cm^{-1} central frequency characteristic of bulk silicon. The Raman peak position (ω_{TO}) and FWHM (Γ) are related to the root-mean-square variation in the bond angle, $\Delta\theta$, of a-Si by the following relations [9]:

$$\frac{\Gamma}{2} = 3.2\Delta\theta + 9.2, \tag{1}$$

$$\omega_{TO} = -2.5\Delta\theta + 505.5. \tag{2}$$

When the structural order starts increasing or the amorphous network relaxes due to the involvement of high-energy ions in the process, the $\Delta\theta$ values decrease. In table 1, the values for thermally evaporated and ion beam sputtered a-Si thin films are given. The evaporated silicon with a central frequency at 472 cm^{-1} has FWHM of 61.37 ± 2 cm^{-1} corresponding to the $\Delta\theta$ values of $13.40 \pm 0.4^\circ$. The ion beam sputtered a-Si thin films, on the other hand, have a Raman central frequency at 483 cm^{-1} and FWHM of 60.08 ± 2 cm^{-1}, and the bond angle variation was $9 \pm 0.21^\circ$ only. Thus, ion beam sputtering aids the relaxation of amorphous network and plays a major role in the local structural ordering.

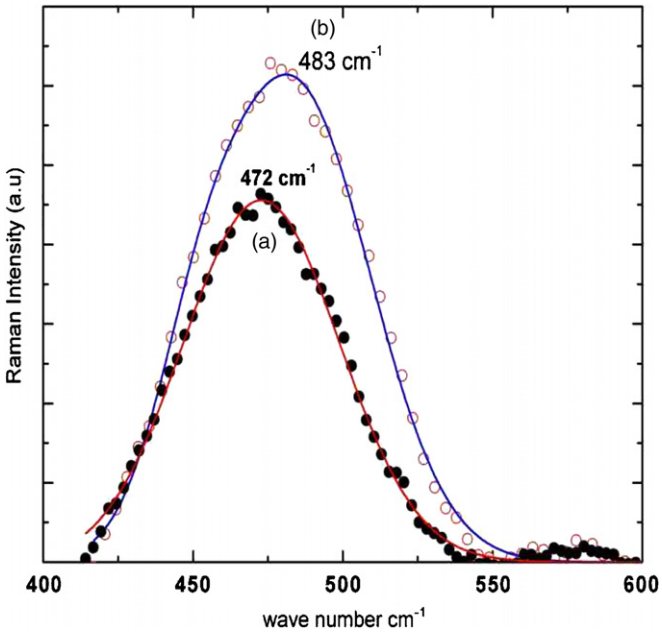

Figure 1. Raman spectra of a-Si thin film: (*a*) thermally evaporated and (*b*) ion beam sputtered.

Table 1. Comparison of the features of the Raman peak exhibited by thermally evaporated and ion beam sputtered a-Si thin films.

Raman peak (ω) (cm^{-1})	FWHM (Γ cm^{-1})	$\Delta\theta$ (deg) From peak broadening	$\Delta\theta$ (deg) From peak position
472 (evap)	61.37 ± 2	6.51061 ± 0.22	13.40 ± 0.4
483 (IBS@600 eV)	60.08 ± 2	6.31515 ± 0.13	9 ± 0.21

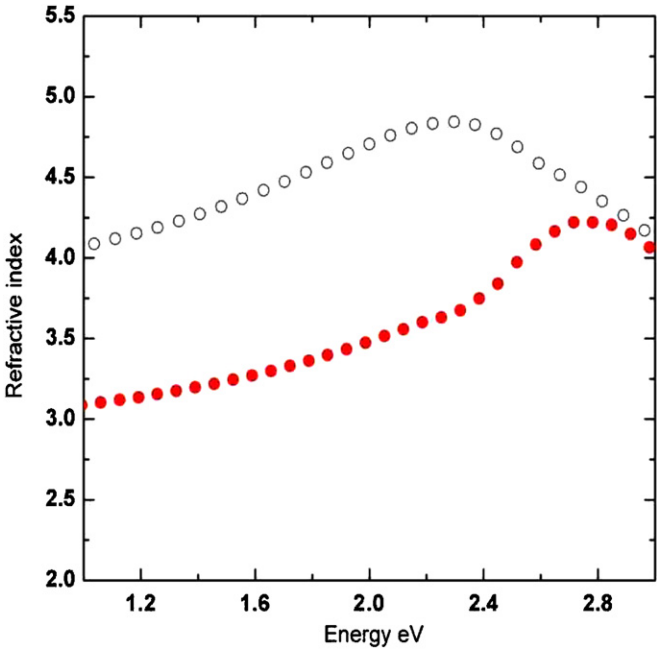

Figure 2. The refractive index behaviour of a-Si thin film of 100 nm thickness deposited at 700 eV (open circles) and 600 eV (solid circles) of incident ion beam energy.

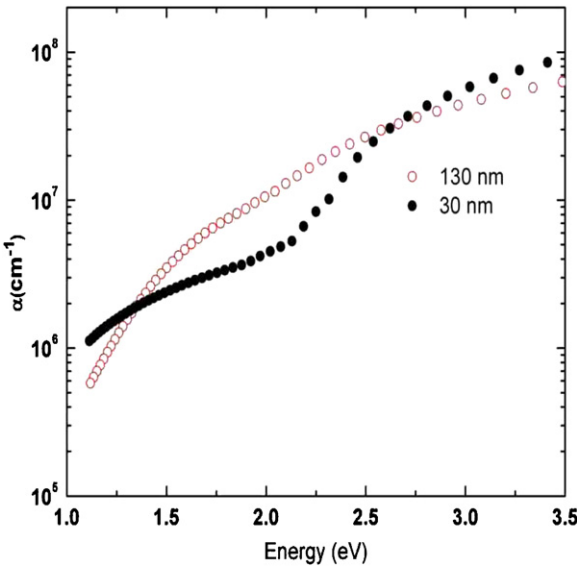

Figure 3. The typical absorption edges of ion beam sputtered a-Si thin films of two different thicknesses.

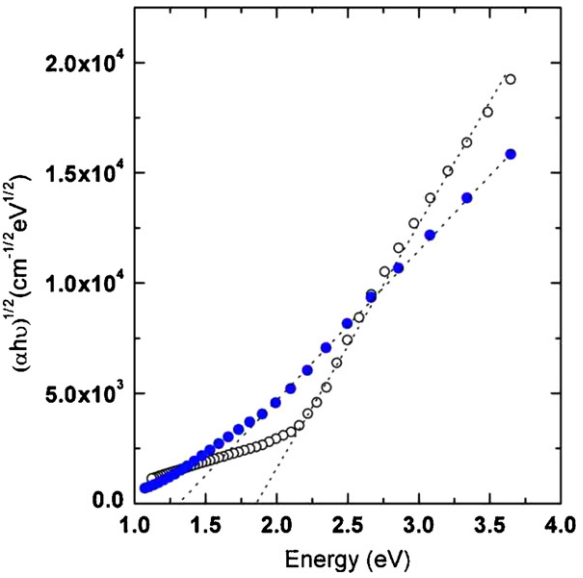

Figure 4. TheTauc gap of ion beam sputtered a-Si thin films of thicknesses 30 and 130 nm.

The index of refraction, n, of the a-Si thin film on glass deposited by ion beam sputtering exhibits a decrease with increase in thickness. This decrease can be attributed to the increase in the Penn gap with relaxation of the strained amorphous network, because the deposition process involves high-energy ions. Typically, with an increase in the thickness, the deficiency in density will reduce resulting in bulk-like refractive index values. When the thickness is increased from 30 nm to 130 nm, the refractive index decreased from 4.4 to 3.7 determined at 1.4 eV as against the bulk silicon value of 3.4 at 1.4 eV in the dispersion-free region. The reported values of refractive index in unhydrogenated a-Si vary from 3.4 to 4.1 [10, 11]. The deviations in the values of n are solely dependent on the method of preparation and conditions of the thin films, and their thermal history. The refractive index was found to depend on the incident ion beam energy as shown in figure 2 for two films of the same thickness deposited at 700 and 600 eV indicating that there is an increase in the refractive index with the beam energy.

These results are in good agreement with a-Si sputter deposited by Richards *et al* [12]. The refractive index values reach a maximum of 4.8 at 2.3 eV for the film deposited at 700 eV and 4.2 at 2.7 eV for the film deposited at 600 eV. The higher refractive index values than the crystalline silicon (c-Si, $n = 3.41$) [13] for these films can be explained in terms of the Penn gap. The Penn gap is a measure of average bond strength. In c-Si, it is 4.8 eV whereas in a-Si, it decreases to ∼3.7 eV due to the weakening of Si–Si bonds [14, 15]. The reduced Penn gap values due to the amorphous nature of the silicon thin films result in a higher refractive index than the c-Si.

The optical absorption coefficient, α, of a 30 nm thin film exhibits a small shoulder between 1.3 and 1.6 eV, which is absent in a 130 nm thick film, as shown in figure 3. This has been interpreted as arising from the maximum in the density of states [16]. This maximum in the density of states at such low energy is due to the divacancies [17] in a-Si, which might correspond to the donor or acceptor levels of such divacancy defects. Two reasons can be attributed for the observed behaviour at higher thickness; once the thickness increases, these vacancies and defects might be saturated or increase in the absorption coefficient shields these effects from showing up in optical investigations.

The plot of $(\alpha h\upsilon)^{1/2}$ versus E in the absorption edge range is displayed in figure 4, and extrapolating the linear region of the curve onto the x-axis gives the optical energy gap. The values for the film thicknesses of 30 nm and 130 nm are 1.8 and 1.3 eV, respectively.

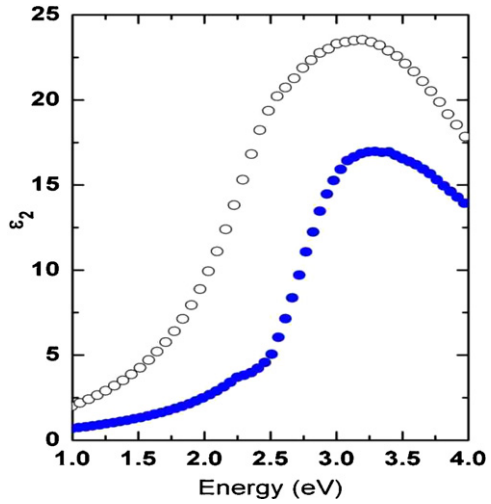

Figure 5. Plots of ε_2 versus photon energy for thin films of thickness 100 nm (open circles) and 60 nm (solid circles).

Table 2. The values of band gap, Urbach energy, deviation in optical gap and refractive index at 1.4 eV for the a-Si thin films of different thickness.

Thickness (nm)	Band gap (eV)	E_U (meV)	ΔE_o (eV)	Refractive index
30	1.8	57	0	4.35
60	1.5	46	0.03	3.85
80	1.67	48	0.37	3.83
100	1.33	47	0.46	3.95
130	1.3	47	0.23	3.52

The so-deduced values of energy gap are reported in table 2 as a function of thickness. The band gap decreases linearly with thickness, and the thickest film of 130 nm reaches a band gap value of 1.3 eV.

With increasing thickness of the film, the band gap energy decreases from 1.8 to 1.3 eV. This suggests that the density of the states is increasing with thickness resulting in decrease of the band gap. The plots of ε_2 versus photon energy for thin films of thickness 100 nm and 60 nm are shown in figure 5. These spectra are typical of amorphous silicon. The variation of ε_2 as a function of photon energy is proportional to the convolution of density of valence and conduction band states separated by the band gap.

In figure 5, the dependence of ε_2 on energy is similar in both the films. But there are key differences in the magnitude and the peak position of ε_2 maxima. The magnitude of decrease is from 23 to 17, as the thickness decreased from 100 nm to 60 nm along with a redshift of ∼0.6 eV in the peak maxima of ε_2. These changes and the increase in the area under the curve suggest an increase of density of states (DOS) with thickness. Savvides [18] stated that assuming the conduction band states were constant, the increase in density of states would result in redistribution of valence band states. This, in turn, will cause the states from the top of the valence band to be pushed deep into the valence band with their contribution appearing at higher energies of $\varepsilon_2(\omega)$. The increase in DOS will decrease the band gap or vice versa. Evidently, in the current study, this is occurring with decrease in thickness and

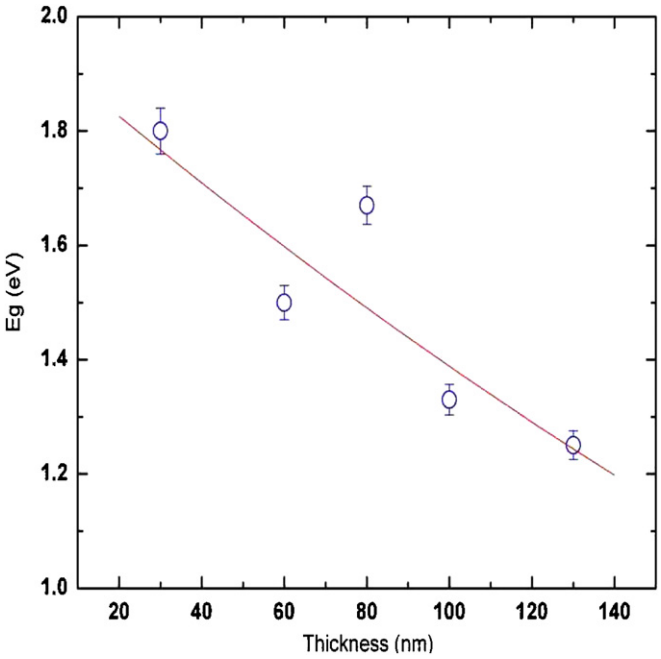

Figure 6. Band gap as a function of thickness of the a-Si thin film.

manifests itself as shown in figure 6, as a decrease in band gap with increase in thickness.

Davis and Mott [19] proposed a model that distinguishes the optical (E_o) and mobility (E_g) gaps in the semiconducting materials. The optical gap was found to be smaller than the mobility gap ($E_g > E_o$). The difference between E_g and E_o gives a measure of the energy range of localized states in the valence and conduction bands. Near the absorption edge, assuming parabolic density of states, the optical-absorption coefficient follows a power law, expressed as

$$\alpha(\omega) = \frac{B(h\omega - E_o)^r}{h\omega}, \tag{3}$$

where B is a constant of the order of 10^5, E_o is the optical energy gap, and r is an index depending on the type of optical transition caused by photon absorption. In crystalline nonmetallic materials, where crystal momentum, k, is conserved, electron transitions obey well-defined selection rules, and r is equal to $\frac{1}{2}$ for allowed direct transitions, $\frac{3}{2}$ for direct forbidden transitions, 2 for allowed indirect transitions and 3 for forbidden indirect transitions. In amorphous materials, the crystal momentum is not conserved, and the momentum selection rules for optical transitions are relaxed. According to Tauc [20], experimental measurements have shown that, in a-Si, α presents an energy dependence of indirect transitions, i.e., $r = 2$, which is a consequence of the well-known fact that silicon has an indirect band gap. We have fixed the value of r to be equal to 2, and the optical-absorption coefficient data were fitted to equation (3) in order to obtain the E_o value. Figure 7 shows the variation of ΔE_o as a function of thickness. With thickness the energy spread of the localized states increases. This increase can be attributed simply to the increase in the density of states with thickness as shown in figure 5.

Apart from the above details, the analysis of the spectrophotometric data gives another parameter called

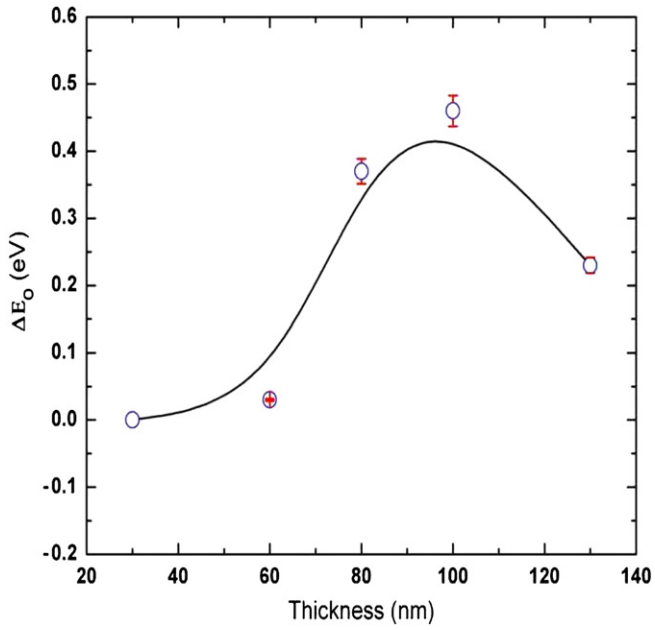

Figure 7. The spread of localized states as a function of thin film thickness.

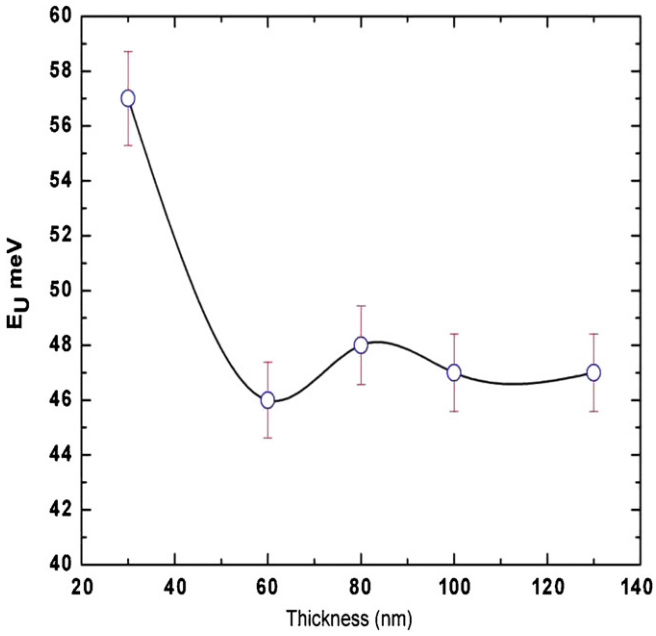

Figure 8. The Urbach energy as a function of thin film thickness.

Urbach energy, E_U, which is a measure of the disorder in the films. This value has contributions resulting from the thermal disorder and static disorder. The E_U values of IBS a-Si thin films are plotted in figure 8, as a function of thickness. After a certain thickness, no significant change is observed in the values of E_U. According to Pankove [21], 1.6 eV should be the ideal band gap of the material for extra-terrestrial solar cell application and that value will decrease when it comes to terrestrial use. Our films show a 1.3 eV band gap, ∼0.2 eV band tailing and 47 meV of Urbach energy at a thickness of 130 nm. Smaller band gap significantly increases the optical absorption, and small band tailings will lower the trap densities.

The Urbach energy value for hydrogenated a-Si prepared by PECVD and other CVD methods ranges from 50 to 150 meV. In the present case, also the Urbach energy value reaches an average of 46 meV, but with relatively much smaller band gap ($E_{g(a\text{-}Si)} = 1.3$ eV) than a-Si:H ($E_{g(a\text{-}Si:H)} = 1.8$ eV).

4. Conclusions

In this work, the linear optical properties of amorphous silicon (a-Si) thin films grown on glass substrates by single ion beam sputtering (IBS) are presented. An attempt is made to distinguish mobility gap E_g and optical gap E_o in IBS a-Si thin films in the analysis of spectrophotometric data. Structural properties of IBS a-Si were explained in terms of optical constants and substantiated using Raman spectroscopy. The band gap value of 1.3 eV suggests that ion beam sputtered a-Si thin films can be explored for photovoltaic applications. Thus, ion beam sputtering has been found to be a viable method for the growth of pure amorphous silicon thin films of high quality along with control over the band gap and microstructure.

Acknowledgments

The authors acknowledge the financial support from the DST-ITPAR program. One of the authors (KUMK) would like to thank the DST-ITPAR for providing a Bose–Romagnosi fellowship to do this work. Facilities provided by the UGC under UPE and SAP programs are gratefully acknowledged. We would like to thank Dr Vasant Sathe from CSR Indore for Raman spectroscopy.

References

[1] Chittick R C, Alexander J H and Sterling H F 1969 *J. Electrochem. Soc.* **116** 77
[2] Brotherton S D 1995 *Semicond. Sci. Technol.* **10** 721
[3] Ayers J R, Brotherton S D and Young N D 1991 *Solid-State Electron.* **34** 671
[4] Staebler D L and Wronski C R 1977 *Appl. Phys. Lett.* **31** 292
[5] Swanepoel R 1983 *J. Phys. E: Sci. Instrum.* **16** 1214
[6] Birgin E G, Chambouleyron I and Martínez J M 1999 *J. Comput. Phys.* **151** 862
[7] Iqbal A and Veprek S 1982 *J. Phys. C: Solid State Phys.* **15** 377
[8] Melinon P *et al* 1998 *J. Chem. Phys.* **108** 4607
[9] Vink R L C, Barkema G T and van der Weg W F 2001 *Phys. Rev.* B **63** 115210
[10] Freeman E C and Paul W 1979 *Phys. Rev.* B **20** 716
[11] Brodsky M H, Title R S, Weiser K and Pettit G D 1970 *Phys. Rev.* B **1** 2632
[12] Richards B S, Lambertz A and Sproul A B 2004 *Thin Solid Films* **460** 247
[13] Green M A and Keevers M 1995 *Prog. Photovolt., Res. Appl.* **3** 189
[14] Phillips J C 1970 *Rev. Mod. Phys.* **42** 290
[15] van Vechten J A 1962 *Phys. Rev.* **128** 2093
[16] Loveland R J, Spear W E and Al-Sharbaty A 1973/74 *J. Non-Cryst. Solids* **13** 55
[17] Watkins G D and Corbett J W 1965 *Phys. Rev.* A **138** 543
[18] Savvides N 1985 *J. Appl. Phys.* **58** 518
[19] Davis E A and Mott N F 1970 *Phil. Mag.* **22** 903
[20] Tauc J, Grigorovivi R and Vancu A 1966 *Phys. Stat. Sol.* **15** 627
[21] Pankove J 1971 *Optical Processes in Semiconductors* (New York: Dover)